THE JOURNAL OF PHYSICAL CHEMISTRY Letters

Letter

pubs.acs.org/JPCL

Surface-Enhanced Femtosecond Stimulated Raman Spectroscopy at 1 MHz Repetition Rates

Lauren E. Buchanan,[†,§] Natalie L. Gruenke,[†,∥] Michael O. McAnally,[†] Bogdan Negru,[†,⊗] Hannah E. Mayhew,[†] Vartkess A. Apkarian,[‡] George C. Schatz,[†] and Richard P. Van Duyne*[,†]

[†]Department of Chemistry, Northwestern University, Evanston, Illinois 60208, United States

[‡]Department of Chemistry, University of California—Irvine, Irvine, California 92697, United States

Supporting Information

ABSTRACT: Surface-enhanced femtosecond stimulated Raman spectroscopy (SE-FSRS) is an ultrafast Raman technique that combines the sensitivity of surface-enhanced Raman scattering with the temporal resolution of femtosecond stimulated Raman spectroscopy (FSRS). Here, we present the first successful implementation of SE-FSRS using a 1 MHz amplified femtosecond laser system. We compare SE-FSRS and FSRS spectra measured at 1 MHz and 100 kHz using both equal pump average powers and equal pump energies to demonstrate that higher repetition rates allow spectra with higher signal-to-noise ratios to be obtained at lower pulse energies, a significant advance in the implementation of SE-FSRS. The ability to use lower pulse energies significantly mitigates sample damage that results from plasmonic enhancement of high-energy ultrafast pulses. As a result of the improvements to SE-FSRS developed in this Letter, we believe that SE-FSRS is now poised to become a powerful tool for studying the dynamics of plasmonic materials and adsorbates thereon.

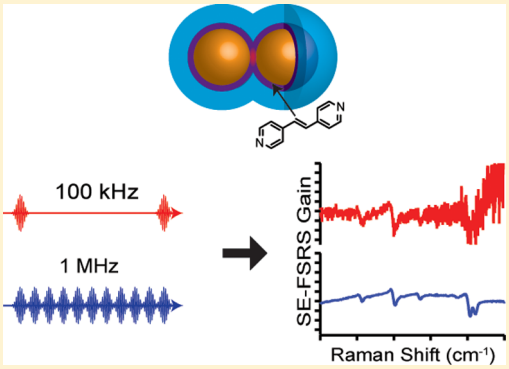

Chemical reactions are described by the motion of atoms as systems evolve from reactants to products. Molecular vibrations, the basis for these atomic motions, thus underlie chemical reaction dynamics. Femtosecond stimulated Raman spectroscopy (FSRS), one of a family of coherent Raman spectroscopies (CRS) that can track molecular vibrations in the time and frequency domain, has emerged as a powerful technique for studying chemical dynamics.[1−3] FSRS is remarkable in its ability to acquire complete vibrational spectra with simultaneous high temporal (10−100 fs) and spectral (5−20 cm^{-1}) resolution, allowing molecular dynamics to be monitored on their most fundamental time scales. FSRS has been applied successfully to a wide variety of chemical and biological systems.[4−7]

Generally, Raman spectroscopies are sensitivity-limited in their application. Because the cross sections for nonresonant Raman scattering are on the order of 10^{-29}−10^{-30} $cm^2\ sr^{-1}\ molecule^{-1}$, typically one is restricted to highly concentrated systems. To this end, the Van Duyne group has developed surface-enhanced femtosecond stimulated Raman spectroscopy (SE-FSRS) in colloidal solutions,[8] while the Apkarian and Potma groups have demonstrated time-resolved SE-CARS on dry-mounted individual nanostructures.[9−11] These approaches take advantage of the electromagnetic (EM) enhancement of the surface fields to increase the CRS signals. In the first demonstration of SE-FSRS, gold nanoparticle assemblies functionalized with *trans*-1,2-bis(4-pyridyl)-ethylene (BPE) exhibited estimated enhancement factors of 10^4−10^6 over FSRS. Furthermore, it was demonstrated that SE-FSRS spectra contain dispersive rather than Lorentzian line shapes,[12] the origin of which was recently explored by Schatz and co-workers.[13]

SE-FSRS has the potential to become a versatile tool for studying ultrafast dynamics of coupled molecule−plasmon systems.[14] For example, recent studies have reported improved efficiencies for plasmonically enhanced photocatalysis and photovoltaic devices, but the mechanism of these enhancements is unclear.[15−18] Additionally, SE-FSRS could prove instrumental in understanding the emerging field of plasmon-driven chemistry, which includes such phenomena as the hot-electron-induced dissociation of hydrogen on gold nanoparticles.[19] As coupling between the molecule and the plasmon has no observable effect on lifetimes of the molecular vibrational coherence required to generate signal,[9,12,20] SE-FSRS is exceptionally well-suited to studying the role of vibrational excited states in plasmonically enhanced photochemistry.

Unfortunately, the development of time-resolved (TR) SE-FSRS has been hindered greatly by sample degradation. The combination of high-energy ultrafast pulses and plasmonic enhancement has been shown to result in melting, fusion, or fragmentation of particles.[21−23] Furthermore, coupled nano-

Received: September 22, 2016
Accepted: November 1, 2016
Published: November 1, 2016

DOI: 10.1021/acs.jpclett.6b02175
J. Phys. Chem. Lett. 2016, 7, 4629−4634

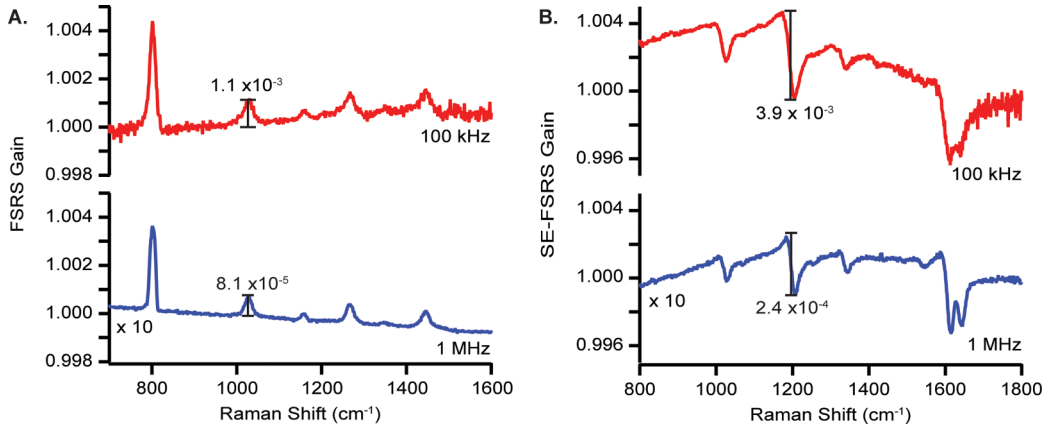

Figure 1. FSRS and SE-FSRS obtained with equal pump average powers: (A) FSRS spectra of CHX obtained with 500 μW of Raman pump at 100 kHz (red) and 1 MHz (blue); (B) SE-FSRS spectra of BPE nanoparticle assemblies obtained with 50 μW of Raman pump at 100 kHz (red) and 1 MHz (blue). Both repetition rates yield FSRS and SE-FSRS spectra with roughly equivalent S/N ratios in the spectral region of 1000−1200 cm^{-1}, but the corrected signal strengths at 100 kHz are approximately 10× higher than those at 1 MHz. The gains of the 1028 cm^{-1} peak of CHX and the 1200 cm^{-1} peak of BPE are labeled.

particles can also undergo irreversible aggregation and sintering[24] which eliminate the highly enhancing hot spots that generate the strongest surface-enhanced Raman scattering (SERS) signals. The gold nanoparticle aggregates used for SE-FSRS were overcoated with silica, an approach shown to improve the thermal, mechanical, and chemical stability of plasmonic substrates.[25−27] However, the SE-FSRS signal obtained of colloidal solutions of these aggregates at 100 kHz still decayed significantly on the time scale of minutes,[8] which hindered attempts to use TR-SE-FSRS to study dynamics. Damage can be mitigated by lowering pulse energies; however, improved sample longevity comes at the cost of decreased signal intensity, leading to longer data acquisition times for equivalent signal-to-noise (S/N) ratios.

Here, we present the first ground-state SE-FSRS spectra obtained at 1 MHz repetition rates. This repetition rate is ten times greater than that of previously published SE-FSRS experiments and 3 orders of magnitude greater than that of typical 1 kHz FSRS experiments, although FSRS studies at repetition rates as high as 80 MHz have been reported.[28,29] We compare ground-state SE-FSRS and FSRS spectra obtained at both 100 kHz and 1 MHz to illustrate the advantages of implementing SE-FSRS at high repetition rates. While the 100 kHz system has been described previously,[8] the 1 MHz system is a new SE-FSRS apparatus. The 1 MHz system, shown in Figure S1, is based on an Yb-doped fiber oscillator/amplifier (Clark-MXR Impulse). The beam diameters of the Raman pump (795 nm, 1 ps) and stimulating probe (approximately 825−950 nm, 30 fs) beams at the sample are adjusted to be ∼55 μm on both systems. Spectra are collected using a Princeton Instruments PIXIS 400BR charge-coupled device (CCD) array. Because of the size of the CCD array, the data collection rate is limited to 500 Hz. Variable pump average powers of 5−500 μW and probe average powers of 0.5−1 μW are used on both systems. The probe powers were chosen to maximize dynamic range filling of the CCD camera, thus reducing shot noise in the collected spectra. Unless otherwise indicated, all spectra are averaged for 30 min. FSRS spectra are presented for cyclohexane (CHX), while SE-FSRS spectra are shown for the gold nanoparticle assemblies used in previous SE-FSRS studies.[8,12] The nanoparticle assemblies consist of approximately 95 nm gold cores aggregated with BPE and subsequently overcoated with silica (Figure S2). A more detailed description of both systems and other experimental considerations is given in the Supporting Information.

First, we compare FSRS and SE-FSRS spectra taken on each system with identical pump and probe average powers. The FSRS spectra of CHX shown in Figure 1A were measured using 500 μW of Raman pump and 0.5 μW of probe. The spectrum obtained at 100 kHz has gain that is approximately 13.5× greater than the one obtained at 1 MHz. In FSRS, Raman gain scales with the peak pump intensity (I_{pump}):

$$\text{Raman gain} = \frac{I_{\text{pump on}}}{I_{\text{pump off}}} = \exp(a\sigma_R czI_{\text{pump}}) \sim 1 + a\sigma_R czI_{\text{pump}} \quad (1)$$

where a is a collection of physical parameters, σ_R the Raman scattering cross section, c the sample concentration, and z the sample path length.[2] Because the gain coefficient is generally small, the FSRS signal scales linearly with the peak intensity of the pump. While it has been demonstrated that the SE-FSRS signals saturate at high pump intensities, likely due to degradation of the samples,[8] the following experiments are performed within the linear regime. While experimental conditions were matched carefully between the two systems, small differences in spatial or temporal overlap can result in slightly different signal strengths. Thus, the difference in Raman gain in Figure 1A matches expectations as the pump pulse energy at 100 kHz is 10× greater than that at 1 MHz for equal average powers. The SE-FSRS signals obtained from the BPE nanoparticle assemblies exhibit an identical pump power dependence (Figure 1B). Both spectra were obtained with 50 μW (50 pJ/pulse at 1 MHz; 500 pJ/pulse at 100 kHz) of Raman pump and 1 μW (1 pJ/pulse at 1 MHz; 10 pJ/pulse at 100 kHz) of probe. As with FSRS, the ratio of the SE-FSRS gains between the two systems does not exactly match that predicted by eq 1; in Figure 1B, gains at 100 kHz are approximately 16× greater than those obtained at 1 MHz. In fact, this trend was observed across all data collected. To compensate for experimental variations between the two systems, an average empirical correction factor of 0.66 will be applied to the 100 kHz S/N values for both FSRS and SE-FSRS in the following sections.

DOI: 10.1021/acs.jpclett.6b02175
J. Phys. Chem. Lett. 2016, 7, 4629−4634

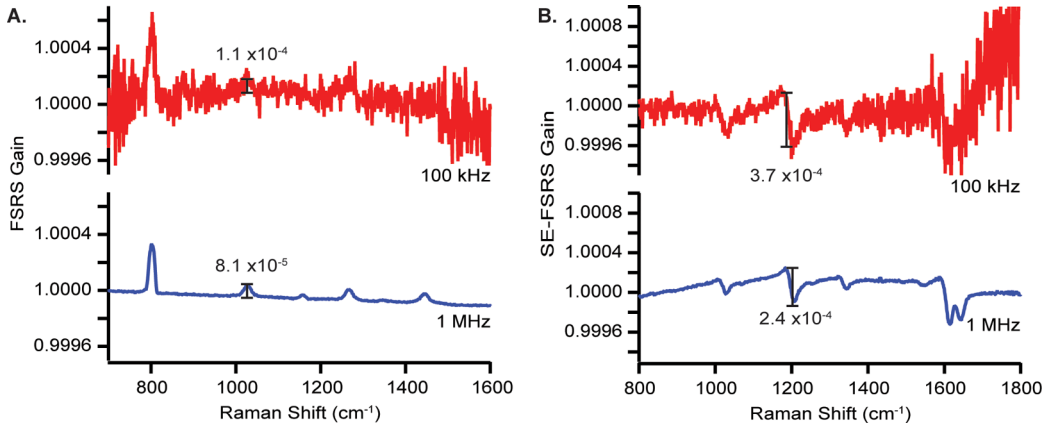

Figure 2. FSRS and SE-FSRS spectra obtained with equal pump pulse energies: (A) FSRS spectra of cyclohexane obtained with 500 pJ/pulse of Raman pump at 100 kHz (red) and 1 MHz (blue); (B) SE-FSRS spectra of BPE nanoparticle assemblies obtained with 50 pJ/pulse of Raman pump at 100 kHz (red) and 1 MHz (blue). Both repetition rates yield similar FSRS and SE-FSRS signal strengths, but the spectra obtained at 100 kHz exhibit noise in the spectral region of 1000−1200 cm^{-1} that is approximately 10× greater than that obtained at 1 MHz. The gains of the 1028 cm^{-1} peak of CHX and the 1200 cm^{-1} peak of BPE are labeled.

To determine the S/N ratio for each SE-FSRS spectrum, we fit the averaged spectrum to a sum of Fano line shape functions[30] superimposed on a broad cubic background, as first implemented in earlier SE-FSRS reports.[12] Each individual vibrational resonance was fit to the function

$$f(\omega) = A\left(\frac{\left(q + \frac{\omega-\omega_0}{\Gamma/2}\right)^2}{1 + \left(\frac{\omega-\omega_0}{\Gamma/2}\right)^2}\right) \quad (2)$$

where A represents the amplitude of the peak; q is the Fano asymmetry parameter that describes the dispersivity of the peak, Γ the line width, and ω_0 the frequency of the molecular vibration. The S/N ratio is defined for a particular peak, i, as the amplitude of the peak divided by the root-mean-square (RMS) value of the noise across the bandwidth of the signal peak.

$$\mathrm{S/N}_i = \frac{A_i}{\mathrm{RMS}_i} \quad (3)$$

The RMS of the noise is calculated from the RMS of the residuals from the Fano fit across the width of the peak. For FSRS spectra, S/N is calculated in a similar manner except each peak is fit to a Lorentzian line shape rather than a Fano line shape. It is important to note that the noise level across each spectrum is highly dependent on the spectral characteristics of the probe (Figure S3). As a result, the 1 MHz spectra have a near constant level of noise across the entire spectral region, while the 100 kHz spectra exhibit the lowest noise in the 1000−1200 cm^{-1} region and rapidly increasing noise toward higher frequencies where reduced filling of the pixels increases the shot noise. Thus, we will compare the S/N for FSRS at the 1028 cm^{-1} band of CHX and the S/N for SE-FSRS at the 1200 cm^{-1} band of BPE where both systems produce the lowest noise.

After 30 min of averaging, the FSRS spectra of CHX (Figure 1A) exhibits a S/N of 12.5 at the 1028 cm^{-1} mode for the spectrum obtained at 1 MHz and a S/N of 20 for the spectrum obtained at 100 kHz. When the 100 kHz S/N is scaled by an empirical correction factor of 0.66, it matches that obtained at 1 MHz. Likewise, the SE-FSRS spectra of the BPE nanoparticle assemblies (Figure 1B) exhibit a S/N of 23 at the 1200 cm^{-1} mode for the spectrum obtained at 1 MHz and a corrected S/N of 24 for the spectrum obtained at 100 kHz. Thus, despite an order of magnitude difference in signal strength between the spectra collected at each repetition rate, the spectra have equivalent S/N ratios. This is not the expected result as the 100 kHz system has 10× more intense signals than the 1 MHz system but should only have $\sqrt{10}$ times greater noise due to the difference in repetition rate. The cause of this discrepancy will be discussed below.

Next, we compare FSRS and SE-FSRS spectra obtained on each system with equal pump pulse energies, rather than average powers. The FSRS spectra of cyclohexane shown in Figure 2A were measured using 50 μW of Raman pump on the 100 kHz system or 500 μW on the 1 MHz system. Thus, the pump pulse energy was 500 pJ/pulse for both cases. Meanwhile, the probe average power was left at 0.5 μW for both systems; this power was chosen because Raman gain is invariant with probe intensity (see eq 1) and using the same average power allowed for equal dynamic range filling of the camera on both systems. While the FSRS spectra have approximately equal gain at both repetition rates, they exhibit a stark difference in noise. The SE-FSRS spectra of the BPE nanoparticle assemblies (Figure 2B) were both obtained using Raman pump pulse energies of 50 pJ/pulse (an average power of 5 μW on the 100 kHz system and 50 μW on the 1 MHz system), while holding the probe power at 1 μW. As with FSRS, the SE-FSRS gains are approximately equivalent for both spectra, but the S/N ratios are dramatically different. As with the comparison performed at equal average powers, an empirical correction factor of 0.66 is required to compare the spectra; the 100 kHz signals are on average 1.5 times stronger than those obtained at 1 MHz.

After 30 min of averaging, the FSRS spectrum of CHX obtained at 100 kHz (Figure 2A) exhibits a S/N of 1.9 at the 1026 cm^{-1} mode. When scaled by the empirical correction factor of 0.66, the S/N is 1.3. This is approximately 10× lower than the S/N of 12 obtained at 1 MHz. Likewise, the SE-FSRS spectrum of the BPE nanoparticle assemblies obtained at 100 kHz (Figure 2B) exhibits a corrected S/N of 2.7 at the 1200 cm^{-1} mode, which is approximately 10× lower than the S/N ratio of 23 obtained at 1 MHz. As predicted, moving to a higher repetition rate system allows SE-FSRS and FSRS spectra to be collected at lower pulse energies with higher S/N than possible using lower repetition rates.

DOI: 10.1021/acs.jpclett.6b02175
J. Phys. Chem. Lett. 2016, 7, 4629−4634

However, the observed improvement in S/N as a function of repetition rate does not match expectations. Signal averaging dictates that the S/N ratio should increase by a factor of $\sqrt{10}$ when collecting signals generated by 10× as many pulses, while we observe a factor of 10 improvement. To uncover the source of this discrepancy, we first examine how S/N scales as a function of signal averaging on each table.

The spectra presented in Figures 1 and 2, which represent 30 min of data averaging, were collected as a set of 100 individual scans. Thus, we can average randomized subsets of these 100 scans and plot the S/N ratios as a function of the number of scans being averaged (Figure 3). On the 1 MHz system, the S/N for both FSRS (cyan) and SE-FSRS (navy) scales properly as $\sqrt{n}$, where n is the number of scans being averaged. However, on the 100 kHz system, the S/N deviates significantly from expected $\sqrt{n}$ scaling and appears to remain nearly constant after only 20 scans (~6 min) for both FSRS (red) and SE-FSRS (maroon). In fact, after 100 scans or 30 min of averaging, the observed S/N is 3−3.5 times smaller than the theoretical value. This difference exactly accounts for the discrepancy in S/N values between the two systems discussed in the previous paragraph. In an attempt to isolate the cause of the empirically asymptotic S/N of the 100 kHz system, we exchanged all data collection electronics between systems including CCD cameras, choppers, and digital delay generators; however, the collected data (not shown) exhibited the same dependence of S/N on the number of scans being averaged.

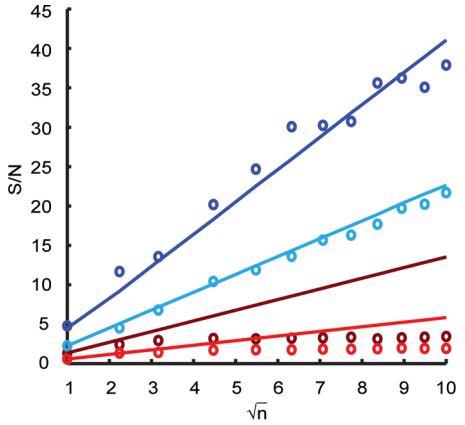

Figure 3. FSRS and SE-FSRS signal averaging at 1 MHz and 100 kHz: Plots of S/N versus $\sqrt{n}$, where n is the number of scans being averaged. Data is shown for SE-FSRS of BPE nanoparticle assemblies obtained at 1 MHz (navy) and 100 kHz (maroon) and for FSRS of CHX obtained at 1 MHz (cyan) and 100 kHz (red). Experimental data are indicated with markers, while solid lines representing $\sqrt{n}$ scalings are added to guide the eye.

To determine whether the noise on the 100 kHz system could be read-out noise-limited rather than shot noise-limited, which would cause signal averaging to fail, we collected FSRS and SE-FSRS spectra at different acquisition rates ranging from 40 Hz to 1 kHz using a PIXIS 100F CCD camera that could accommodate higher repetition rates. Once again, the same S/N scaling was observed. Having eliminated all elements of the data collection process as possible culprits, we conclude that the problem must originate with the 100 kHz laser itself. While the source of the signal averaging problem in the 100 kHz system is unresolved, ultimately this does not detract from the results presented in this Letter.

The SE-FSRS spectra presented herein were obtained at average powers as low as 1/40th of those used in previously published work, which used hundreds of microwatts of pump power on a 100 kHz system.[8] At these powers, half of the SE-FSRS signal was lost after 5 min of data collection; extended exposure to pulsed irradiation at high powers resulted in a decrease of the near-infrared extinction of the Au nanoparticle assemblies. These results suggested a destruction of the highly enhancing multicore particles that contribute most strongly to the SE-FSRS signal. However, any structural changes to the nanoparticles were too small to be observed by transmission electron microscopy on the few nanometer length scale. To probe the extent of sample damage when using high average powers at either 100 kHz or 1 MHz, we measured SE-FSRS spectra for 30 min using 500 μW of Raman pump (corresponding to pulse energies of 5 nJ at 100 kHz or 500 pJ at 1 MHz). At this power, the signal at 100 kHz does not increase significantly over the signal obtained using 50 μW (Figure S4);[8] only an 8% increase in signal strength is observed despite an order of magnitude difference in pump power. In contrast, 500 μW at 1 MHz still falls within the linear regime of the pump power dependence of SE-FSRS gain. As a result, the signal magnitudes are now comparable, despite an order of magnitude difference in pulse energies, and the spectra display improved S/N at 1 MHz due to increased averaging. In fact, at 500 μW the S/N ratio now exceeds 375 after 30 min of averaging. In Figure 4, we show a time evolution of the SE-FSRS gain signal. The signal from the 100 kHz system decreases to less than half of its initial value over the course of 30 min, while the signal from the 1 MHz system remains constant. Thus, using a higher repetition rate laser system allows us to collect SE-FSRS at high enough pump powers to achieve optimal gain and S/N without any apparent damage to the samples. Furthermore, at these powers, less than a minute of averaging is sufficient to achieve a S/N of 41 (Figure S5). Hence, the use of higher repetition rate systems reduces the amount of time necessary to collect a well-averaged SE-FSRS

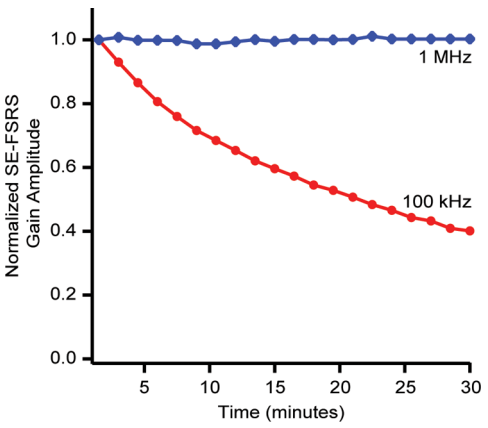

Figure 4. Monitoring sample degradation via signal decay in SE-FSRS experiments. While significant loss of SE-FSRS signal is observed on the minute time scale at 100 kHz (red), the signal obtained at 1 MHz (blue) remains constant throughout 30 min of data collection. SE-FSRS spectra were collected using 500 μW of pump (corresponding to pulse energies of 5 nJ at 100 kHz or 500 pJ at 1 MHz), and the gain amplitudes are shown for the 1200 cm^{-1} mode of BPE, normalized to the initial value for each experiment. The other BPE Raman modes decrease in amplitude at the same rate.

DOI: 10.1021/acs.jpclett.6b02175
J. Phys. Chem. Lett. 2016, 7, 4629−4634

spectrum, subsequently reducing the time necessary to collect TR-SE-FSRS data in future experiments.

In summary, we have successfully acquired the first SE-FSRS spectra obtained at 1 MHz repetition rates. We have shown that SE-FSRS, which requires low pulse energies to avoid sample degradation, is better implemented with high repetition rate laser systems. We can now obtain SE-FSRS spectra at 1 MHz with comparable gain as at 100 kHz and with improved S/N. The ability to collect spectra at powers that are orders of magnitude lower than those of previous SE-FSRS experiments opens up new classes of plasmonic substrates for use. Up to this point, SE-FSRS measurements have proved successful only on silica-coated nanoparticles like those used in this Letter. While the silica coating mitigates sample degradation, it also limits the variety of samples that can be used. With the 1 MHz system, SE-FSRS can potentially be applied to a wide range of plasmonic systems, including uncoated colloids and two-dimensional nanosphere lithographic substrates, which will be explored in future experiments. Ultimately, we wish to incorporate time-resolution and use SE-FSRS to study the dynamics of coupled molecule−plasmon systems. TR-FSRS studies generally require significant averaging at a multitude of time steps, which necessitates that samples cannot degrade over the length of the scan. While flowing samples have been used to circumvent sample degradation in nonenhanced FSRS experiments,[4] this approach requires a large amount of sample and is often impractical for use with plasmonic samples that are difficult or expensive to prepare in bulk. At 1 MHz, well-averaged SE-FSRS spectra can be obtained at powers that do not cause damage over the course of 30 min, which is sufficient time to conduct a time-dependent study based on analogous FSRS measurements. This represents a significant step toward using SE-FSRS in studies of chemical dynamics. The improved S/N ratio at 1 MHz will further facilitate such efforts because the lower noise floor requires less averaging for small transient signals to be resolved. As a result of the improvements to SE-FSRS developed in this Letter, we believe that SE-FSRS is poised to become a powerful tool for studying the dynamics of coupled molecule−plasmon systems.

■ ASSOCIATED CONTENT

Supporting Information

The Supporting Information is available free of charge on the ACS Publications website at DOI: 10.1021/acs.jpclett.6b02175.

Additional data and experimental details (PDF)

■ AUTHOR INFORMATION

Corresponding Author

*E-mail: vanduyne@northwestern.edu. Phone: 847-491-3516. Fax: 847-491-7713.

Present Addresses

[§]L.E.B.: Department of Chemistry, Vanderbilt University, Nashville, TN 37235.

[∥]N.L.G.: Department of Chemistry, University of California Berkeley, Berkeley, CA 94720.

[⊗]B.N.: Department of Chemistry, Sonoma State University, Rohnert Park, CA 94928.

Notes

The authors declare no competing financial interest.

■ ACKNOWLEDGMENTS

L.E.B., N.L.G., M.O.M., H.E.M., V.A.A., G.C.S., and R.P.V.D. were supported by the National Science Foundation Center for Chemical Innovation dedicated to Chemistry at the Space−Time Limit (CaSTL) Grant CHE-1414466. B.N. was supported by the National Science Foundation Grant CHE-1506683. N.L.G., M.O.M., and H.E.M. acknowledge support from the National Science Foundation Graduate Research Fellowship Program (DGE-0824162). All instrumentation used in these experiments was purchased by the National Science Foundation Center for Chemical Innovation dedicated to Chemistry at the Space−Time Limit (CaSTL) Grant CHE-1414466. We thank STA Technologies for providing the nanoantennae.

■ ABBREVIATIONS

FSRS, femtosecond stimulated Raman spectroscopy; SE-FSRS, surface-enhanced femtosecond stimulated Raman spectroscopy; SERS, surface-enhanced Raman scattering; BPE, *trans*-1,2-bis(4-pyridyl)-ethylene; SECARS, surface-enhanced coherent anti-Stokes Raman spectroscopy; S/N, signal-to-noise

■ REFERENCES

(1) Kukura, P.; McCamant, D. W.; Mathies, R. A. Femtosecond Stimulated Raman Spectroscopy. *Annu. Rev. Phys. Chem.* **2007**, *58*, 461−488.

(2) McCamant, D. W.; Kukura, P.; Yoon, S.; Mathies, R. A. Femtosecond Broadband Stimulated Raman Spectroscopy: Apparatus and Methods. *Rev. Sci. Instrum.* **2004**, *75*, 4971−4980.

(3) Dietze, D. R.; Mathies, R. A. Femtosecond Stimulated Raman Spectroscopy. *ChemPhysChem* **2016**, *17*, 1224−1251.

(4) Fang, C.; Frontiera, R. R.; Tran, R.; Mathies, R. A. Mapping GFP Structure Evolution during Proton Transfer with Femtosecond Raman Spectroscopy. *Nature* **2009**, *462*, 200−205.

(5) Kukura, P.; McCamant, D. W.; Yoon, S.; Wandshneider, D. B.; Mathies, R. A. Structural Observation of the Primary Isomerization in Vision with Femtosecond-Stimulated Raman. *Science* **2005**, *310*, 1006−1009.

(6) Brown, K. E.; Veldkamp, B. S.; Co, D. T.; Wasielewski, M. R. Vibrational Dynamics of a Perylene−Perylenediimide Donor−Acceptor Dyad Probed with Femtosecond Stimulated Raman Spectroscopy. *J. Phys. Chem. Lett.* **2012**, *3*, 2362−2366.

(7) Magnanelli, T. J.; Bragg, A. E. Time-Resolved Raman Spectroscopy of Polaron Pair Formation in Poly(3-Hexylthiophene) Aggregates. *J. Phys. Chem. Lett.* **2015**, *6*, 438−445.

(8) Frontiera, R. R.; Henry, A.-I.; Gruenke, N. L.; Van Duyne, R. P. Surface-Enhanced Femtosecond Stimulated Raman Spectroscopy. *J. Phys. Chem. Lett.* **2011**, *2*, 1199−1203.

(9) Yampolsky, S.; Fishman, D. A.; Dey, S.; Hulkko, E.; Banik, M.; Potma, E. O.; Apkarian, V. A. Seeing a Single Molecule Vibrate through Time-Resolved Coherent Anti-Stokes Raman Scattering. *Nat. Photonics* **2014**, *8*, 650−656.

(10) Crampton, K.; Zeytunyan, A.; Fast, A.; Tork Ladani, F.; Alfonso-Garcia, A.; Banik, M.; Fishman, D. A.; Potma, E. O.; Apkarian, V. A. Ultrafast Coherent Raman Scattering at Plasmonic Nanojunctions. *J. Phys. Chem. C* **2016**, *120*, 20943−20953.

(11) Zeytunyan, A.; Crampton, K. T.; Zadoyan, R.; Apkarian, V. A. Supercontinuum-Based Three-Color Three-Pulse Time-Resolved Coherent Anti-Stokes Raman Scattering. *Opt. Express* **2015**, *23*, 24019−24028.

(12) Frontiera, R. R.; Gruenke, N. L.; Van Duyne, R. P. Fano-Like Resonances Arising from Long-Lived Molecule-Plasmon Interactions in Colloidal Nanoantennas. *Nano Lett.* **2012**, *12*, 5989−5994.

(13) McAnally, M. O.; McMahon, J.; Van Duyne, R. P.; Schatz, G. C. Coupled Wave Equations Theory of Surface-Enhanced Femtosecond Stimulated Raman Scattering. *J. Chem. Phys.* **2016**, *145*, 094106.

DOI: 10.1021/acs.jpclett.6b02175
J. Phys. Chem. Lett. 2016, 7, 4629−4634

(14) Gruenke, N. L.; Cardinal, M. F.; McAnally, M. O.; Frontiera, R. R.; Schatz, G. C.; Van Duyne, R. P. Ultrafast and Nonlinear Surface-Enhanced Raman Spectroscopy. *Chem. Soc. Rev.* **2016**, *45*, 2263−2290.
(15) Kochuveedu, S. T.; Jang, Y. H.; Kim, D. H. A Study on the Mechanism for the Interaction of Light with Noble Metal-Metal Oxide Semiconductor Nanostructures for Various Photophysical Applications. *Chem. Soc. Rev.* **2013**, *42*, 8467−8493.
(16) Hou, W.; Cronin, S. B. A Review of Surface Plasmon Resonance-Enhanced Photocatalysis. *Adv. Funct. Mater.* **2013**, *23*, 1612−1619.
(17) Ueno, K.; Misawa, H. Surface Plasmon-Enhanced Photochemical Reactions. *J. Photochem. Photobiol., C* **2013**, *15*, 31−52.
(18) Zhang, Z.; Deckert-Gaudig, T.; Deckert, V. Label-Free Monitoring of Plasmonic Catalysis at the Nanoscale. *Analyst* **2015**, *140*, 4325−4335.
(19) Mukherjee, S.; Zhou, L.; Goodman, A. M.; Large, N.; Ayala-Orozco, C.; Zhang, Y.; Nordlander, P.; Halas, N. J. Hot-Electron-Induced Dissociation of H2 on Gold Nanoparticles Supported on SiO2. *J. Am. Chem. Soc.* **2014**, *136*, 64−67.
(20) Voronine, D. V.; Sinyukov, A. M.; Hua, X.; Wang, K.; Jha, P. K.; Munusamy, E.; Wheeler, S. E.; Welch, G.; Sokolov, A. V.; Scully, M. O. Time-Resolved Surface-Enhanced Coherent Sensing of Nanoscale Molecular Complexes. *Sci. Rep.* **2012**, *2*, 891.
(21) Haller, K. L.; Bumm, L. A.; Altkorn, R. I.; Zeman, E. J.; Schatz, G. C.; Van Duyne, R. P. Van. Spatially Resolved Surface Enhanced Second Harmonic Generation: Theoretical and Experimental Evidence for Electromagnetic Enhancement in the near Infrared on a Laser Microfabricated Pt Surface. *J. Chem. Phys.* **1989**, *90*, 1237−1252.
(22) Fujiwara, H.; Yanagida, S.; Kamat, P. V. Visible Laser Induced Fusion and Fragmebtation of Thionicotinamide-Capped Gold Nanoparticles. *J. Phys. Chem. B* **1999**, *103*, 2589−2591.
(23) Link, S.; Burda, C.; Mohamed, M. B.; Nikoobakht, B.; El-Sayed, M. A. Laser Photothermal Melting and Fragmentation of Gold Nanorods: Energy and Laser Pulse-Width Dependence. *J. Phys. Chem. A* **1999**, *103*, 1165−1170.
(24) Eah, S. K.; Jaeger, H. M.; Scherer, N. F.; Lin, X. M.; Wiederrecht, G. P. Femtosecond Transient Absorption Dynamics of Close-Packed Gold Nanocrystal Monolayer Arrays. *Chem. Phys. Lett.* **2004**, *386*, 390−395.
(25) Li, X.; Lee, J.; Blinn, K. S.; Chen, D.; Yoo, S.; Kang, B.; Bottomley, L. A.; El-sayed, M. A. Environmental Science High-Temperature Surface Enhanced Raman Cell Materials †. *Energy Environ. Sci.* **2014**, *7*, 306−310.
(26) Wang, X.; Luo, A.; Liu, H.; Zhao, N.; Liu, M.; Zhu, Y.; Xue, J.; Luo, Z.; Xu, W. Nanocomposites with Gold Nanorod/Silica Core-Shell Structure as Saturable Absorber for Femtosecond Pulse Generation in a Fiber Laser. *Opt. Express* **2015**, *23*, 22602−22610.
(27) Sung, J.; Kosuda, K. M.; Zhao, J.; Elam, J. W.; Spears, K. G.; Van Duyne, R. P. Stability of Silver Nanoparticles Fabricated by Nanosphere Lithography and Atomic Layer. *J. Phys. Chem. C* **2008**, *112*, 5707−5714.
(28) Dobner, S.; Cleff, C.; Fallnich, C.; Gross, P. Interferometric Background Reduction for Femtosecond Stimulated Raman Scattering Loss Spectroscopy. *J. Chem. Phys.* **2012**, *137*, 174201.
(29) Beier, H. T.; Noojin, G. D.; Rockwell, B. A. Stimulated Raman Scattering Using a Single Femtosecond Oscillator with Flexibility for Imaging and Spectral Applications. *Opt. Express* **2011**, *19*, 18885−18892.
(30) Fano, U. Effects of Configuration Interaction on Intensities and Phase Shifts. *Phys. Rev.* **1961**, *124*, 1866−1878.

DOI: 10.1021/acs.jpclett.6b02175
J. Phys. Chem. Lett. 2016, 7, 4629−4634